Earth Syst. Sci. Data, 18, 5759–5771, 2026
https://doi.org/10.5194/essd-18-5759-2026

Open Access Earth System Science Data

Global dataset of storm surges and extreme sea levels for 1950–2024 based on the ERA5 climate reanalysis

Natalia Aleksandrova[1], **Jelmer Veenstra**[1], **and Sanne Muis**[1,2]

[1]Department of Hydrodynamics and Forecasting, Deltares, Delft, 2629 HV, the Netherlands
[2]Department of Water and Climate Risk, Faculty of Science, Vrije Universiteit Amsterdam, Amsterdam, 1081 HV, the Netherlands

Correspondence: Natalia Aleksandrova (natalia.aleksandrova@deltares.nl)

Received: 5 August 2025 – Discussion started: 3 September 2025
Revised: 4 May 2026 – Accepted: 6 July 2026 – Published: 4 August 2026

Abstract. Extreme sea levels, generated by storm surges and high tides, can cause coastal flooding and erosion. Global datasets have been instrumental in mapping extreme sea levels and associated societal risks. Harnessing the backward extension of the ERA5 reanalysis, we present a dataset containing timeseries of tides and storm surges based on a global hydrodynamic model covering the period 1950–2024. This is an extension of a previously published dataset that covered a shorter period (1979–2018). Using this dataset, we estimate extreme sea levels globally. Validation shows good agreement between observed and modelled sea levels, with the level of agreement for the extended dataset being very similar to that of the previously published dataset. The extended 75-year dataset allows for a more robust estimation of return periods, often resulting in smaller uncertainties than its 40-year precursor. This underscores the necessity for long timeseries and the strength of long-term modelling enabled by the ERA5 reanalysis extension. The present dataset can be used for assessing flood risk, climate variability and climate changes. The timeseries dataset is openly accessible at https://doi.org/10.24381/cds.a6d42d60 (Muis et al., 2025a) and the statistical indicators are available on Zenodo at https://doi.org/10.5281/zenodo.14671593 (Muis et al., 2025b).

1 Introduction

Extreme sea levels, driven by the combination of mean sea level, tides, storm surges and waves (Woodworth et al., 2019), can drive coastal flooding. Global reanalysis of extreme sea levels have improved our understanding of the driving mechanisms of coastal flooding at large-scales (Hinkel et al., 2021). The reanalysis datasets have been used to estimate exceedance probabilities, which are valuable input for coastal flood risk assessment that are used for both disaster risks reductions and climate change mitigation and adaptation (Tiggeloven et al., 2020). One of the first global reanalysis dataset of still sea levels, called the Global Tide and Surge Reanalysis (GTSR) dataset was published in 2016 (Muis et al., 2016). This dataset was based on surge simulations of Global Tide and Surge Model version 2.0 (GTSMv2.0) forced with ERA-Interim, which were superimposed with tide simulations of the FES2012 model (Carrere et al., 2012). The hydrodynamic approach has a higher accuracy than previous global return periods of extreme sea levels that used simplified parametric models to estimate storm surges (Muis et al., 2017; Hinkel et al., 2014). Moreover, a modelling approach provides an improved spatial coverage compared to previous quasi global assessment that were based on sparse dataset of observations (Menéndez and Woodworth, 2010; Fang et al., 2014). In 2020, an updated reanalysis dataset was published based on GTSMv3.0 forced with the ERA5 climate reanalysis (Muis et al., 2020). Model development allowed to include tides from the same model, and thereby account for non-linear interaction between tides and storm surge which has shown to be important in shallow regions with a large tidal range (Arns et al., 2020). The ERA5 reanalysis has a much higher spatial and temporal resolution than its predecessor ERA-Interim (31 vs. 78 km; 1 vs. 6 h). This has greatly improved the performance of global surge modelling, particularly in regions prone to tropical cyclones (Muis et al., 2020; Dullaart et al., 2020).

GTSM timeseries of still water levels generated using climate reanalysis data, presented in the GTSR (ERA-Interim) and GTSM-ERA5 datasets, have been widely used in coastal hazards research, for example in the analysis of individual historical events both in terms of the height of water levels (Dullaart et al., 2020) and their impact (Koks et al., 2023). They have also been used to investigate the event footprint and spatial dependencies (Enriquez et al., 2020; Li et al., 2023), as well as the influence of climate variability on surge levels (Muis et al., 2018) and in comparisons with GTSM driven by climate models (Muis et al., 2023a). GTSR data was used to study the potential links between storm surges and shoreline changes globally (Ghanavati et al., 2023). The GTSM-ERA5 reanalysis has also been used to remove the meteorological influence from the historical observed sea-level trends for the Dutch coast, which helped to reveal an acceleration of the sea-level rise (Stolte et al., 2023). The GTSM reanalysis datasets have also been used to assess the dependency between storm surge and other flood drivers (Couasnon et al., 2020; Ridder et al., 2020; Nasr et al., 2021; Camus et al., 2021) and its influence on (compound) flooding (Couasnon et al., 2020; Ikeuchi et al., 2017; Eilander et al., 2020). Since GTSM is a barotropic depth-averaged model, some coastal processes are not well-captured. Several studies have improved this by supplementing the reanalysis with other data. This includes combining the return periods of still water levels with estimates of wave setup based on the significant wave height from ERA5 (Kirezci et al., 2020) and with mean sea levels from ocean reanalysis to better capture the mean sea level response (Muis et al., 2018; Treu et al., 2024).

The timeseries of water levels are used to derive statistical parameters, such as percentiles and return periods. Different methods, such as annual maxima and peaks-over-threshold have been applied in different studies: the GTSR dataset was analysed using annual maxima (Muis et al., 2016), while peaks-over-threshold method was applied to GTSM-ERA5 (Muis et al., 2023a). While determining the appropriate threshold can be challenging at global-scale, peaks-over-threshold method can extract multiple peaks per year and makes more efficient use of the available data. Extreme value analysis have large uncertainties when applied in broad-scale studies (Wahl et al., 2017), but the resulting return periods are nevertheless useful for first-order large-scale assessments of coastal flood hazard and risk (Tiggelhoven et al., 2020; Lincke and Hinkel, 2018; Brown et al., 2018), including infrastructure and cultural heritage sites (Reimann et al., 2018; Verschuur et al., 2023).

The latest GTSM-ERA5 reanalysis dataset covers the period 1979 to 2018 (Muis et al., 2023a). The length of 40 years is relatively short considering the large decadal variability (Lobeto and Menendez, 2024). Recently, the ERA5 climate reanalysis was extended backwards to 1940 (Bell et al., 2021; Hersbach et al., 2023), seamlessly joining with the dataset covering 1979 to the present. The quality of the reanalysis was improved by assimilating additional conventional observations, as well as through making better use of early satellite data. While trend analysis before the satellite-era should be carefully done (Tadesse et al., 2022), the ERA5 dataset extension allows to also extend the storm surge reanalysis dataset derived using GTSM. Such an extended dataset may reduce the uncertainty of the extreme values fit and would allow to quantity decadal variability more accurately.

In this paper, we present an extension of the previous surge reanalysis dataset that covered the period 1979–2018 (Muis et al., 2023a). We use the same modelling chain, which consists of GTSMv3.0 in combination with tidal and meteorological forcing as well as annual mean sea level. Leveraging the backward extension of ERA5 dataset, we extend the surge sea level dataset to span a period from 1950 to 2024, resulting in the GTSM-ERA5-E dataset. To achieve this, a portable and easily repeatable workflow was developed, that can be used to deploy Global Tide and Surge Model (GTSM) on a high-performance computing (HPC) cluster. We describe the workflow that was used to produce the dataset, validate the dataset against observed sea levels, and we show the effect of longer records on the extreme value analysis and associated uncertainties.

2 Methodology

The workflow consists of three main steps that are visualized in Fig. 1. The first step is the *model simulations* (blue colours in Fig. 1), which consists of pre-processing input data, running GTSM, and post-processing of output data into timeseries per geographical location. The second step is the *analysis* of the timeseries data on a global scale using extreme value statistics (yellow colours in Fig. 1). The third step is the *validation* of the modelled water levels against observed water levels at selected stations (green colours in Fig. 1).

The workflow is realized through a combination of Python and bash scripts. All the simulations are run on the Dutch National Supercomputer Snellius, which makes use of SLURM job scheduler. Each step of the workflow is semi-automated where the bash scripts are used to submit specific jobs. The data processing and analysis are largely done with Python 3 using the *xarray* package (Hoyer and Hamman, 2017), whereas the model simulations make use of the Delft3D Flexible Mesh software (Kernkamp et al., 2011).

2.1 Model simulations

We use the recent backward extension of the ERA5 climate reanalysis (Hersbach et al., 2023) to simulate time series of still water levels from 1950 to 2024. Hourly wind speed and atmospheric pressure (u10, v10, and msl) are downloaded from the Climate Data Store (CDS) by Copernicus Climate Change Service (C3S). In a preprocessing step, we adjust the

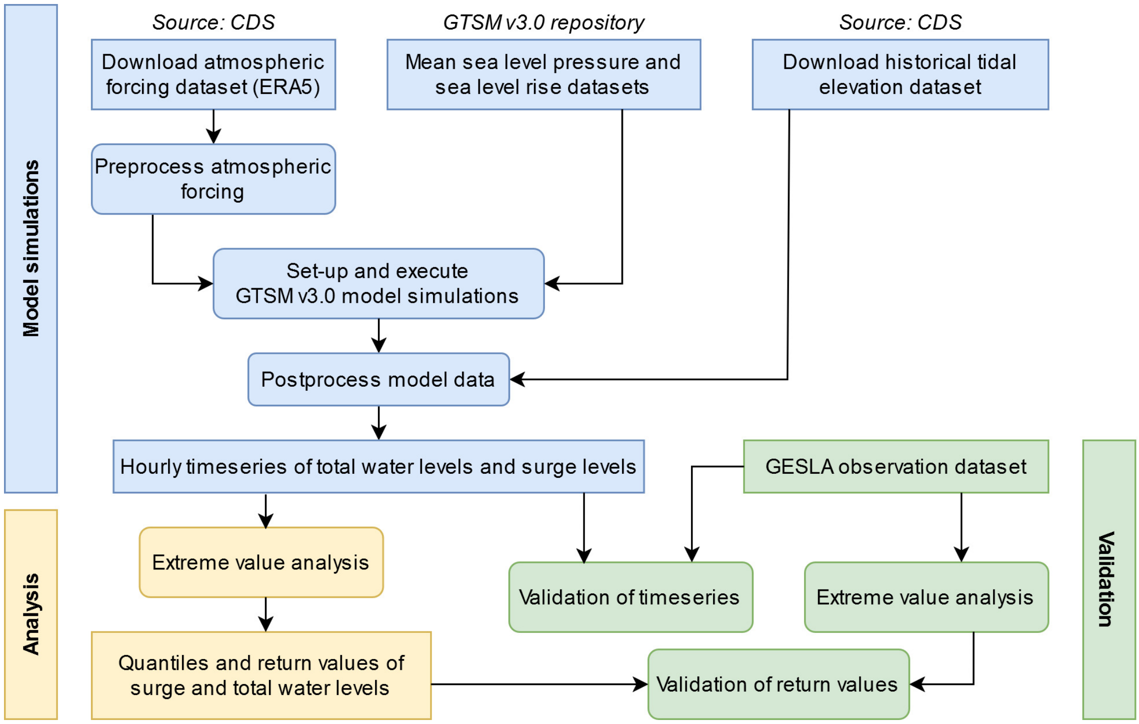

Figure 1. Flow chart of the main workflow that was used to generate the GTSM-ERA5-E water level reanalysis.

format of the meteorological data to make it compatible with the hydrodynamic modelling software. Sea level rise is included in the simulations by using a spatially-varying dataset of annual mean sea levels (Muis et al., 2023b). The underlying sea level rise data was compiled using the probabilistic model of Le Bars (2018) and is defined at a spatial resolution of $1° \times 1°$; the data for 1950–2016 is based on observations, and the data from 2016 onwards is based on projections from the mean ensemble Fifth Assessment Report (AR5) of the Intergovernmental Panel on Climate Change (IPCC, 2013). The detailed methodology behind the sea level rise dataset is provided in the supporting information for the previous publication where this dataset was utilized (Muis et al., 2023a), the same sea level rise dataset is used for the extension, in order to maintain continuity. After the model is initialized, the pressure and wind speed forcing from ERA5 is applied, and to harmonize the vertical reference of the water levels the yearly mean sea level pressure over 1986–2005 is subtracted via an additional correction in the form of a negative pressure field (Muis et al., 2023b).

We simulate tides and storm surges with GTSMv3.0 using the same configuration as described in previous work (Muis et al., 2020). The GTSMv3.0 is a depth-averaged hydrodynamic model with global coverage that dynamically simulates tides and storm surges. GTSMv3.0 is based on the unstructured Delft3D Flexible Mesh software (Kernkamp et al., 2011). We make use of a singularity container, which allows us to run Delft3D Flexible Mesh on any HPC cluster in a simple, portable, and reproducible way. GTSM has a spatially varying resolution, which goes up to 2.5 km at the global coast and 1.25 km at the European coast. The bathymetry is derived from various sources: General Bathymetric Chart of the Ocean (GEBCO) with a 30 arcsec resolution (Weatherall et al., 2015), European Marine Observation and Data Network (EMODnet) at 250 m resolution in Europe (EMODnet Bathymetry Consortium, 2018), and Bedmap2 for the bathymetry under and thickness of the permanent ice shelves in Antarctica (Fretwell et al., 2013). These datasets are internationally recognized, openly available, and provide full global coverage. However, it must be noted that the GEBCO dataset has a relatively low resolution and can carry significant uncertainty in data-scarce regions. This limitation is inherent to the global modelling based on open data. The model has no open boundaries. Tides are induced by including tide generating forces using a set of 60 frequencies (tidal constituents), defined in Delft3D Flexible Mesh software and selected to achieve optimal trade-off between accuracy and computational efficiency. Storm surges are generated by the transfer of momentum from the wind to the water, with an additional contribution by the changes in atmospheric pressure through the inverse barometer effect. We use the Charnock formulation (Charnock, 1955) with a drag coefficient of 0.041 to estimate the wind stress at the ocean surface. To minimize the data storage requirements, we use a set of 44 734 output locations (Muis et al., 2020) that include $\sim$ 18 000 coastal points every $\sim$ 10–50 km along the coast and ocean points on a semiregular grid at a resolution that varies between 0.25 and 5°. The model runs are set up using an automatized workflow by creating separate yearly model simulations with a spin-up time of 15 d, and a timestep of 10 min. Using a parallel setup with 128 cores and 224 GB of RAM, each 1-year simulation takes approximately 1 d to complete. Subsequently the output from the yearly simulations can be combined to obtain the full dataset by removing the spin-up part of the simulation.

In the postprocessing step we compute storm surge levels as a difference between a total water level simulation and a tide-only simulation. For this we use a tide-only simulation that is already available from CDS and covers the same period (Muis et al., 2025a). In addition, the NetCDF4 file format is optimized, the data for the spin-up period is removed, unnecessary variables are dropped, and metadata is prescribed. Datasets with timeseries of hourly mean water levels and daily maximum water levels are derived directly from the 10 min timeseries of water levels.

2.2 Data analysis

The data analysis consists of two steps. First, we compute monthly and annual minima and maxima for water levels and surge heights. Then, we detrend the timeseries by removing the annual means from the still water level dataset to achieve a stationary dataset without sea level rise. Based on this detrended dataset, we compute percentiles and return values. To obtain the latter, we apply extreme value analysis (EVA) to estimate the exceedance probabilities. Following Wahl et al. (2017), we apply the Peak Over Threshold (POT) approach and we fit the Generalized Pareto Distribution (GPD) on the peaks that exceed the 99th percentile water level, then we derive estimates for various return periods, including confidence intervals. We use a 72 h window for the de-clustering of the events to ensure their independence. We use the Maximum Likelihood Estimation (MLE) to fit the GPD parameters, with the Monte Carlo method used to define confidence intervals. This analysis is realized using the *pyextremes* package (Bocharov, 2023). The analysis is done for the extended period (1950–2024), as well as the original period (1979–2018) to enable comparison between datasets of different duration.

2.3 Validation

To validate the dataset, we compare the modelled still water levels with high-frequency observations of sea levels from the tide gauge stations in the Global Extreme Sea Level Analysis (GESLA) dataset, version 3 (Haigh et al., 2023). The validation is performed for two periods: 1979–2020 (recent period, where GESLA data is available) and 1950–1978 (backward extension period). We only use the tide gauge stations where there is less than 25 % of data missing in either of the two periods, and remove duplicated stations, keeping the longest records among the duplicates. Additionally, the data records are filtered according to the data quality flag value to only use records where no data quality issues are indicated. This selection results in 107 stations that can be used for extreme value analysis, where each station has a matching location in the GTSM-ERA5-E dataset (within 10 km distance). The data coverage in the resulting observational dataset used for data validation is 96.2 % for 1950–1978, and 97.5 % for 1979–2020 (on average across stations).

Each observation record is resampled to hourly data. In order to match the vertical reference of the GTSM-ERA5 dataset, the mean water level in 1986–2005 is subtracted from each record, and daily, monthly and annual maxima are calculated. The model performance of GTSM-ERA5-E is evaluated by comparing observed and modelled values for daily, monthly and annual maxima. For each station, the model data is filtered to only include the periods where observation data is available, and resampled to daily, monthly and annual maxima timeseries. We use the mean bias (MB), the mean absolute error (MAE), and the mean absolute percentage error (MAPE) to compare the modelled and observed data. Next to that, we calculate the root mean square error (RMSE) and Pearson correlation coefficient across timeseries for each station. Mean and standard deviation of these parameters across stations provide an indication of the model performance as compared to observations. Comparing these metrics between the two validation periods (1950–1978 and 1979–2020) provides insight into the differences in performance between the original period and the backward extension.

3 Data records

The timeseries dataset of total water levels and surge heights for all output points for 1950–2024 based on ERA5 reanalysis data are publicly accessible at the Copernicus Climate Change Service Climate Data Store (CDS) (Muis et al., 2025a). This data is made available at several temporal resolutions: 10 min, hourly means and daily maxima. The newly added data extends the already available dataset that covered the period 1979–2018. This dataset includes a global selection of coastal and ocean output points ($>$ 43 000 points, see Fig. 3 for an indication of coverage). The timeseries data of total water levels includes sea level rise (updated yearly), and uses the local mean sea level over 1986–2005 as a vertical reference. Mean sea level fields are available as a separate variable in the dataset, which could be used to detrend the total water levels.

The descriptive statistics of still water levels (percentiles and extreme values) derived from the GTSM-ERA5-E dataset for each output point are publicly accessible at the Zenodo repository (Muis et al., 2025b). This includes percentiles (1st, 5th, 10th, 25th, 50th, 75th, 90th, 95th, 99th) and extreme values corresponding to different return periods (1, 2, 5, 10, 25, 50, 75 and 100 years). The extreme values include the best-fit values, 5 %–95 % confidence intervals and descriptors of the extreme value fits (shape, scale and location parameters). The descriptive statistics are calculated over the full period of GTSM-ERA5-E dataset, and are based on detrended timeseries of hourly total water levels, removing the effect of sea level rise.

4 Technical validation

4.1 Still water level statistics validation

A comparison between the modelled and observed values at 107 observation stations globally is shown in Table 1. The comparison is presented for the recent time period (1978–2020) and the backward extension time period (1950–1978). In general, there is a good agreement of the validation metrics between the two periods, indicated by very similar values for Pearson correlation of 0.6 for annual maxima (with standard deviation across stations being 0.24 and 0.27 for the recent period and backward extension period respectively). Also the RMSE shows very similar values for both periods. For both periods there is a similar degree of underestimating annual maxima, by 0.10–0.11 m on average (standard deviation across stations of 0.25–0.26 m). The only notable difference is in the MAPE of the monthly maxima, which is larger in the backward extension period (annual maxima MAPE does not show a similar difference). A closer look at individual stations' statistics reveals that large differences in monthly maxima MAPE are observed only for 5 stations (not limited to a specific region). These differences in performance can have various sources, including changes in tide gauge location or changes in record quality further back in time. Overall this validation demonstrates that the extended time period has the same level of agreement with observations as the recent time period, with nearly all performance metrics for the monthly and annual maxima timeseries showing very small differences. This suggests that the backward extension of the ERA5 dataset for the period 1950–1978 is well suited for use in the modelling of global water levels, with resulting data having comparable quality to the GTSM-ERA5 dataset that covers the period 1979–2018, at least in the regions covered by this validation.

Figure 2 shows the spatial distribution of the statistical metrics for the annual maxima from Table 1 across stations. This figure also shows the global coverage of filtered GESLA being limited to specific regions with long-term records, mainly clustered in Western Europe, North America and Japan. The general underestimation of extremes is consistent with findings from previous work (Muis et al., 2016, 2020; Dullaart et al., 2020) and can be attributed to the underestimation of extreme winds in ERA5 in combination with the model's resolution. Especially storm surges induced by tropical cyclones, which have steep pressure gradients within a relatively small area, will be impacted by the low model resolution and are likely to be underestimated. This underestimation is visible in Fig. 2 as the largest negative bias and RMSE shown at the East coast of the USA, where the annual maxima are dominated by tropical cyclone activity.

Table 1. Model performance of the GTSM-ERA5 in the extended period (1950–1978) and the period without the backward extension (1979–2020), comparing still water levels to tide gauge observations (selection of 107 GESLA-3 long tide gauge records). The values are presented as mean across stations with standard deviation (in brackets).

Data	Metric	GTSM-ERA5 extension 1950–1978	GTSM-ERA5 1979–2020
Monthly maxima	Mean bias [m]	−0.03 (0.24)	−0.03 (0.26)
	MAE [m]	0.18 (0.18)	0.19 (0.19)
	MAPE [%]	33.8 (79.0)	20.5 (14.8)
	RMSE (m)	0.21 (0.18)	0.22 (0.18)
	Pearson corr. coef.	0.74 (0.17)	0.73 (0.17)
Annual maxima	Mean bias [m]	−0.11 (0.25)	−0.10 (0.26)
	MAE [m]	0.20 (0.19)	0.21 (0.19)
	MAPE [%]	14.2 (8.9)	14.5 (8.9)
	RMSE (m)	0.22 (0.19)	0.23 (0.19)
	Pearson corr. coef.	0.60 (0.24)	0.60 (0.27)

In addition to the impact of the dataset extension on water level statistics, Fig. 3 also demonstrates the GTSM-ERA5 water levels and storm surge height comparison to observations for several specific major storm events in the extension period (1950–1978) at three tide gauges with long-term records. This includes the storm surge caused by the extratropical storm in the North Sea in 1968, hurricane Carla (1961) that impacted the United States, and typhoon Marie (1954) that impacted Japan. The storm surge signal was obtained from the tide gauge records by removing the tidal component using *hatyan* software (Veenstra, 2026).

The storm surge caused by the North Sea storm in 1968 at the Esbjerg tide gauge is the fourth highest water level in 1950–2024 and it is well-captured in the GTSM-ERA5-E with good agreement both in terms of timing and magnitude of the maximum water levels. For the Galveston tide gauge, water levels during storm Carla are the second highest over the 1950–2024 record (second to Hurricane Ike in 2008); the magnitude and timing of the storm surge are well-represented by the GTSM-ERA5-E, with differences in the decay of the elevated water levels after the storm surge peak – in the observations the water levels stay elevated for a longer period. In the case of typhoon Marie and the Hosojima tide gauge (highest measured water level in 1950–2024), GTSM-ERA5-E captures the timing of the maximum water levels well, but underestimates the total water levels. When comparing the modelled and measurement-derived surge timeseries, the peak surge height is underestimated for the North Sea storm (−9 %) and typhoon Marie (−14 %), but is overestimated (+14 %) for Hurricane Carla.

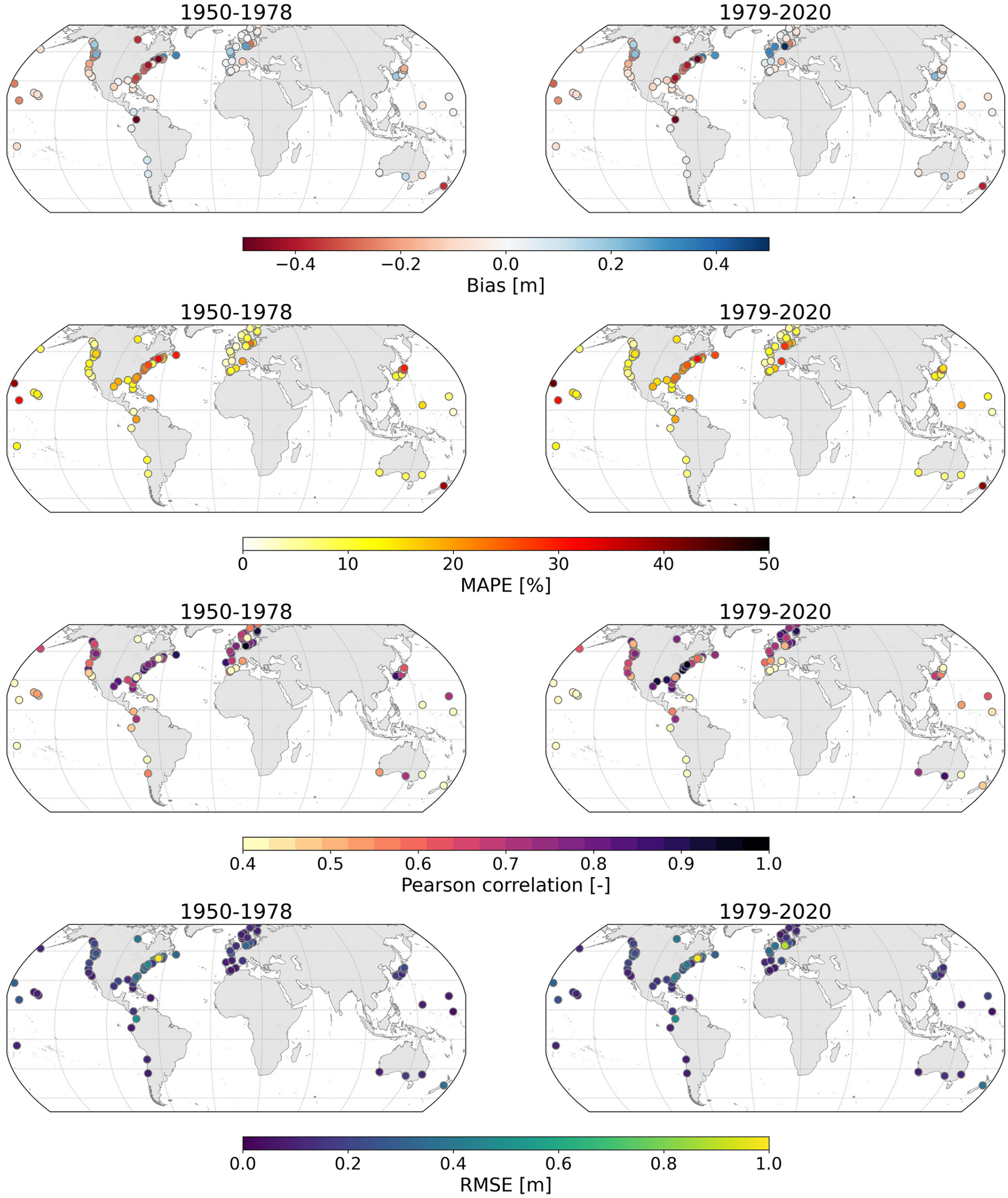

Figure 2. Global map showing the comparison between the modelled and observed annual maxima water levels for two periods: 1950–1978 (left) and 1979–2020 (right) for the following metrics (from top to bottom): bias, mean absolute percentage error (MAPE), Pearson correlation coefficient and RMSE.

4.2 Impact of dataset extension on water level statistics and extreme return values

The global water level statistics derived from the extended GTSM-ERA5-E dataset are compared to those derived from the original GTSM-ERA5 dataset to understand the impact and potential benefits of the longer timeseries. To quantify the difference in surges between the backward extension and the more recent period, we compare the surge height statistics by calculating the mean annual maxima values based the 30-year timeseries for 1950–1979 and 1995–2024. The difference is shown in Fig. 4, where it can be seen that in by far the most areas the difference is minor (within 0.1 m), indicating that the surge statistics are reasonably consistent between the extended and the original periods. There are, however, several areas where larger differences are visible. In general, there are negative differences in high-latitude regions, such

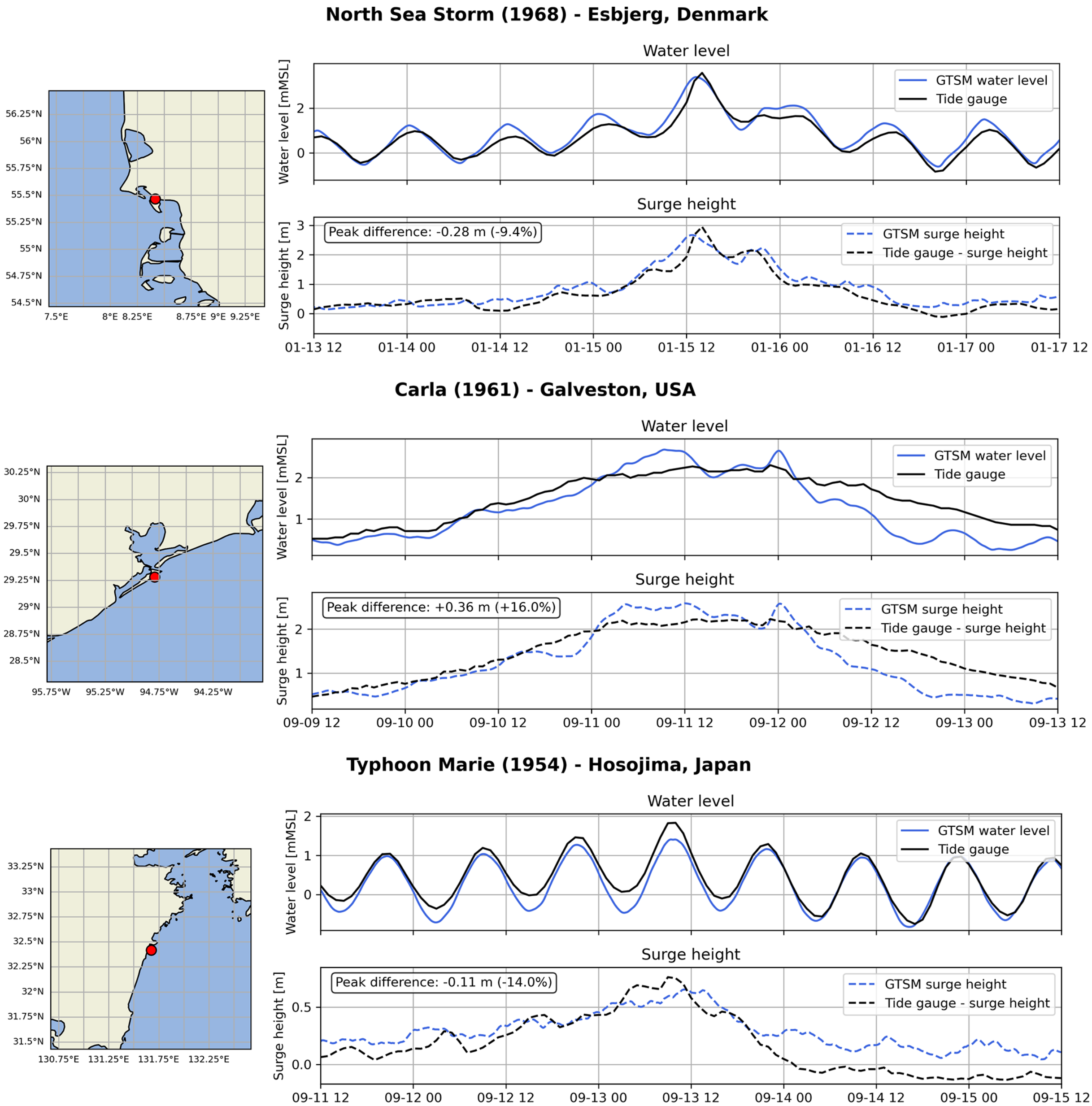

Figure 3. Comparison of water levels and surge heights from the GTSM-ERA5-E database and observations from the GESLA archive, shown for historical storm events, including the North Sea storm in 1968, hurricane Carla (1961), and typhoon Marie (1954).

as Antarctica and Northern Europe, and positive differences difference for most of the rest of the globe. It is not clear what drives these differences in surge statistics, and the extended GTSM-ERA5 dataset provides an opportunity for further research to explore these differences across the full 75-year period. It is possible that some of these differences are caused by climate variability (Lobeto and Menendez, 2024). In regions with limited historical weather records, the differences can also be influenced by varying ability of ERA5 backward extension to represent historical extreme storm events.

The availability of longer timeseries is potentially useful for a more robust estimation of extreme values. Figure 5 shows the 100-year return values based on the extended dataset (75 years) and the original dataset (40 years). Differences are generally within 0.2 m, although increases and decreases up to 0.5 m occur locally. The largest increases in the 100-year return values are seen in regions affected by tropical cyclones. This could be linked to the occurrence of tropical cyclones that have relatively low probabilities and that are most likely under-sampled when a shorter period is considered. This includes regions such as Mozambique, Philip-

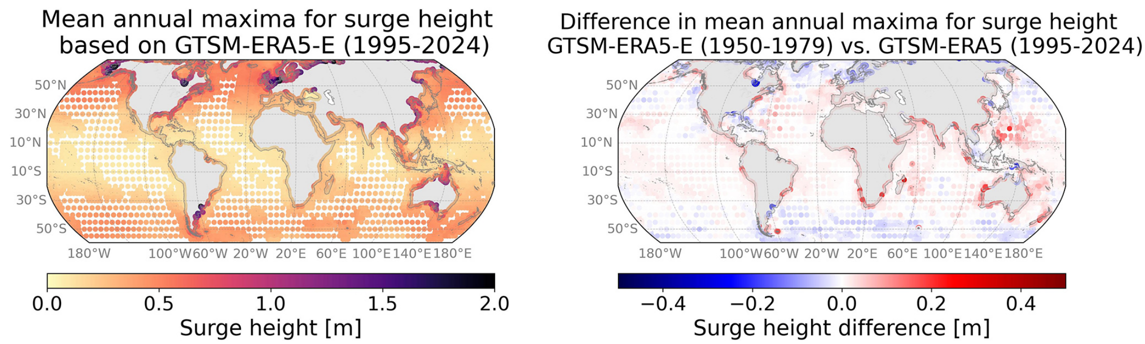

Figure 4. Global maps showing the difference in mean annual maxima values for surge height calculated based on a 30-year period at the start of the GTSM-ERA5-E backward extension dataset (1950–1979) and a recent 30-year period (1995–2024).

pines, Caribbean, and northern Australia. There are also regions where there is a decrease, such as Northern Europe and parts of the northern coast of the United States. It is known that even on relatively large timescales of several decades there can be significant variability in storm surge extremes (Lobeto and Menendez, 2024). Future research could investigate these trends in detail and quantify the influence of interannual variability as well as climate change.

For 85 % of all timeseries data output locations in the dataset, the width of the 5 %–95 % confidence intervals for extreme return values of total water levels decreases when using the full length of GTSM-ERA5-E dataset in the extreme value analysis. The width of the confidence interval corresponding to the 100-year return values is reduced by 13 % on average across all output points. Figure 6 shows the difference in confidence interval width for the 100-year return values, demonstrating that for most regions globally the confidence intervals become narrower. An increase in the width of the confidence intervals is observed at clusters of locations in tropical cyclone regions. This is expected, considering that the sample size is too small and robust estimates of return period for those regions require thousands of years of tropical cyclone activity (Lin and Emanuel, 2016; Bloemendaal et al., 2020).

Additional insight into the differences between GTSM-ERA5 and GTSM-ERA5-E is obtained by considering the extreme value analysis results for individual locations. Figure 7 shows return value plots for eight locations globally, including the best-estimate values and confidence intervals based on the extended and original datasets, as well as based on observations. It shows that the effect of using longer records differs from station to station. At some locations, such as Esbjerg, Bergen and Galveston, the best-estimate return values from GTSM-ERA5-E and original GTSM-ERA5 are very similar, but the confidence interval becomes narrower when using GTSM-ERA5-E due to the longer time series. At other locations, such as Fremantle, Hosojima, Cuxhaven and Montauk, higher extreme return values are obtained when using longer timeseries – at these locations the extension of the time series allows the inclusion of more severe storms that were not part of the original 1979–2018 dataset. For locations with low storm surge activity, such as Newlyn, the return values do not change a lot between the datasets. This overview highlights the range of possible changes in estimated extreme water levels that can result from using a dataset covering a longer period of time. While for most (seven out of the eight) locations shown here, the return periods based on GTSM-ERA5-E are still within the confidence bounds of those based on GTSM-ERA5, the difference for higher return periods can be considerable. Hence, the plots indicate that in both tropical and extra-tropical regions the length of 40 years of data (as in the previous version of GTSM-ERA5) may not always be sufficient to robustly estimate return periods. It must be noted that the quality of the extreme value analysis fits based on the peak-over-threshold method with fixed threshold selection varies from location to location. The chosen single-distribution fit is relatively stiff, and is only partially affected by the highest extremes in the data. In the examples illustrated in Fig. 7 this is particularly visible for locations affected by tropical cyclones, such as Montauk and Galveston.

The comparison between GTSM-ERA5-derived and observations-derived extreme values in Fig. 7 shows that for most stations there is a vertical bias. This offset can be seen both for the fitted extreme value distribution (blue and black solid lines) as well as the individual extremes (blue and black dots). These biases are expected in a global model, and can be resulting from inaccuracies in the tidal signal (due to low resolution of the model and complexity of some of the coastlines, as well low accuracy of bathymetric information in some regions) and underestimations of surge magnitudes (which can be a result of underestimations of wind speeds in ERA5, especially for tropical storms, as well as due to inaccurate bathymetric information in some regions). However, the observed frequency of the individual extremes matches with the GTSM-ERA5-E dataset, which can be seen by comparing the blue and black dots in Fig. 7. The extended dataset can help to better identify the return periods of spe-

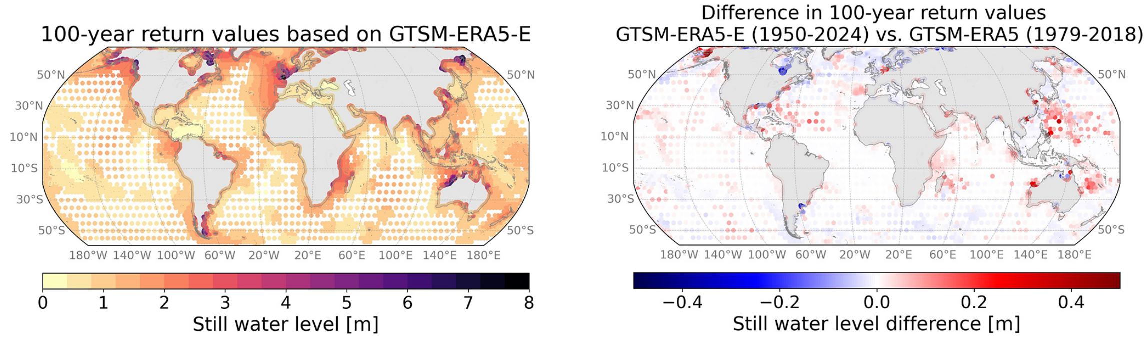

Figure 5. Global maps showing the 100-year return values based on 1950–2024 water levels (left) and a difference between 100-year return values between the GTSM-ERA5-E dataset (1950–2024) and the original GTSM-ERA5 dataset (1979–2018). The difference plots are calculated by subtracting the GTSM-ERA5 100-year water levels from the GTSM-ERA5-E 100-year water levels.

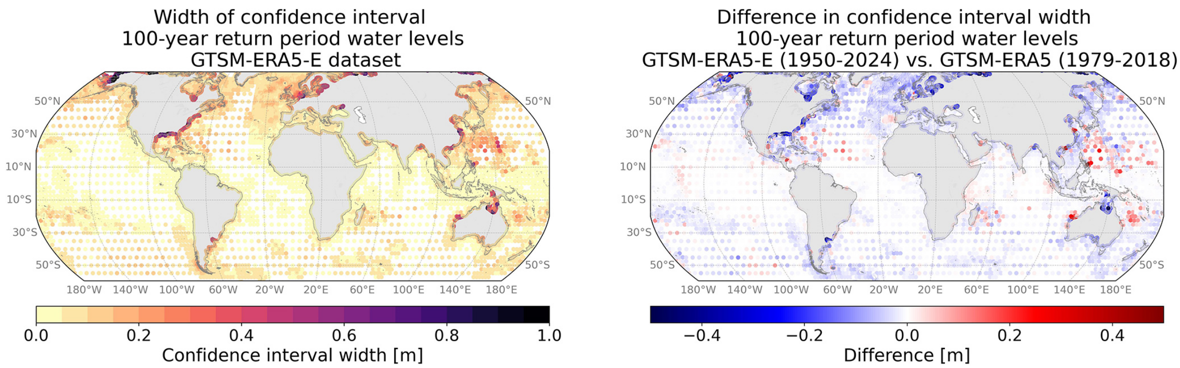

Figure 6. Overview of differences in confidence intervals between the 100-year return values of water levels derived from GTSM-ERA5-E and GTSM-ERA5 datasets.

cific events, compared to the original shorter dataset. For example, at the Esbjerg tide gauge, the most extreme event in the GTSM-ERA5 was initially given a return period of 40 years, while based on the longer record length it is assigned a return period of 70 years, both based on GTSM-ERA5-E and observations.

5 Data availability

The dataset of total water levels and surge height time-series described in this manuscript can be accessed at the Copernicus Climate Change Service Climate Data Store under DOI https://doi.org/10.24381/cds.a6d42d60 (Muis et al., 2025a). The descriptive statistics of total water levels (percentiles and extreme values) derived from the timeseries dataset can be accessed at Zenodo under DOI https://doi.org/10.5281/zenodo.14671593 (Muis et al., 2025b).

6 Code availability

The Delft3D Flexible Mesh software that was used for the hydrodynamic modelling is openly available for download at https://download.deltares.nl/en/download/delft3d-fm/ (last access: 22 July 2026). A singularity container was used to run in a high-performance computing environment: https://oss.deltares.nl/web/delft3dfm/get-started (last access: 22 July 2026). All code (Python and bash scripts) that was used to generate the datasets described here are publicly available via GitHub and preserved at Zenodo under DOI https://doi.org/10.5281/zenodo.14671593 (Muis et al., 2025b).

7 Conclusions

This paper presents an extended dataset of oceanic and coastal water levels and surge heights globally, derived using the ERA5 reanalysis from 1950 to the present. This dataset is methodologically consistent with the previous version of the dataset covering time period of 1979 to 2018. The extended dataset spans a period of 75 years, offering the basis for deriving long-term statistics and extremes, as well as analysing specific past events. An accompanying dataset of water level statistics globally is presented in this paper. The accuracy of the dataset is analysed through statistical validation against a global dataset of water level observations (GESLA) and through the more detailed look at three individual past se-

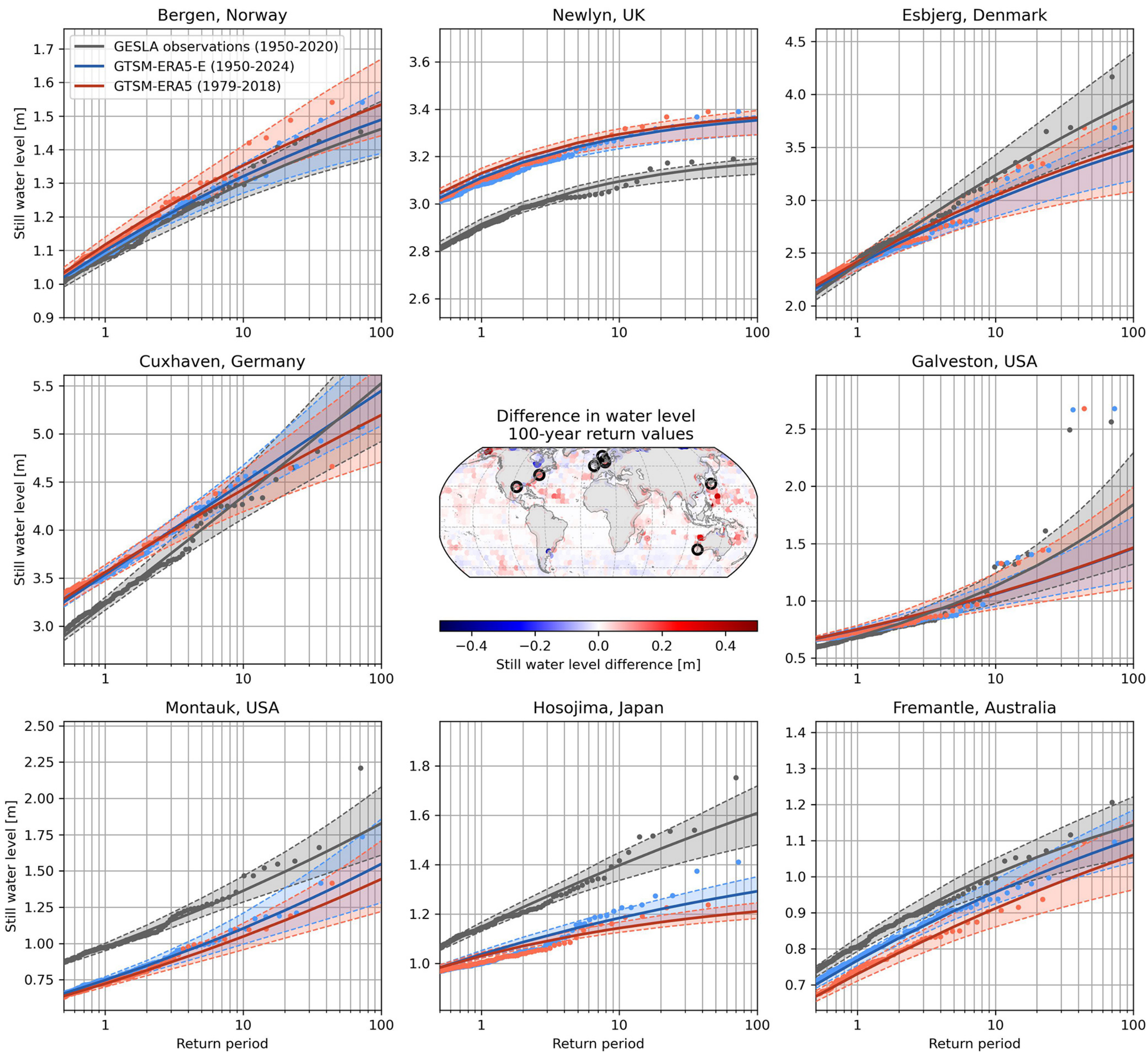

Figure 7. Extreme value analysis return value plots for multiple coastal locations globally demonstrating the difference between extremes estimated based on the GTSM-ERA5-E dataset (1950–2024) and shorter original GTSM-ERA5 dataset (1979–2018), as well as based on tide gauge observations (1950–2020). The shaded areas indicate the 5 %–95 % confidence intervals.

vere storm events covered by the dataset extension as well as comparisons of extreme value analysis results.

There are several aspects of the presented dataset that are advised to consider when using this dataset. While the dataset offers significant extension of the temporal coverage, caution is advised when using the ERA5-based dataset to derive water level statistics in areas prone to tropical cyclones, because the record length of 75 years can be still insufficient to account for low-probability events (Lin and Emanuel, 2016). Next to that, it is important to keep in mind the limitations of a global dataset. First, it is well-reported in literature that the intensity of extreme storms and tropical cyclones in particular will be underestimated in ERA5 (Dulac et al., 2024), which will also underestimate storm surge levels (Bloemendaal et al., 2019). Second, as a global model, GTSM does not capture local storm surges in very complex coastal areas, the observed surges can be found to be much higher than modelled values. Also the low accuracy of global bathymetry data may negatively affect the accuracy of our results. Therefore, we recommend that if users want to use the global data for a regional study, they need to consider the specific context and evaluate the suitability of the modelling assumptions.

The validation of the GTSM-ERA5-E dataset for 1950–1978 relies on long-term tide gauge records, which are geographically sparse and are mainly restricted to Europe, North America and Japan, and lack data for e.g. Africa, South America and South Asia. At the same time, the ERA5 backward extension also relies on data assimilation of long-term weather records (in the pre-satellite era, before 1979), which are similarly unevenly distributed. It is plausible that the quality of ERA5 data in terms of capturing extreme events is higher in the regions with the highest density of observations. Based on the validation we conclude that the backward extension can be used to increase the length of time series for used in extreme value analysis, although caution is advised when using this dataset to estimate long-term trends since the quality of ERA5 is likely to be improving over time and affect the trend analysis.

The extended dataset can be used for a more robust estimation of extreme water levels, where the long record length can contribute to reducing confidence intervals and improving the accuracy of high return period point estimates. The extreme value statistics of total water levels calculated in this study are intended for first-order global overview of extremes. Extreme value analysis performed at a global scale using fixed thresholds carries considerable uncertainty. In local studies on water level and surge extremes it is strongly recommended to perform more accurate extreme value analysis based on the available water level and surge timeseries, where individual fits can be evaluated and adjusted by setting appropriate thresholds. In future research, the use of more advanced and flexible extreme value analysis techniques could be applied to the entire global dataset in order utilize the longer record length towards obtaining more accurate estimates globally.

The dataset provides a valuable resource for assessing flood risks in coastal regions. The time series data can be used as input for flood models to investigate historical events, while the extreme return values can inform flood risk assessments (Tiggeloven et al., 2020; Lincke and Hinkel, 2018). In wave-dominated regions, we recommend to combine the GTSM-derived water levels with wave setup computed based on the ERA5 wave reanalysis (Kirezci et al., 2020). We also acknowledge that in some cases the sea level reanalysis can be improved by combining it with mean sea level reconstructions (Treu et al., 2024) that account for ocean processes that are not resolved by GTSM. For regional to local-scale application both statistical and dynamic downscaling could be explored.

Author contributions. All authors contributed to code development. S.M. drafted the initial version of the manuscript. Data analysis and validation of data were carried out by N.A. under supervision of S.M.

Competing interests. The contact author has declared that none of the authors has any competing interests.

Disclaimer. Publisher's note: Copernicus Publications remains neutral with regard to jurisdictional claims made in the text, published maps, institutional affiliations, or any other geographical representation in this paper. The authors bear the ultimate responsibility for providing appropriate place names. Views expressed in the text are those of the authors and do not necessarily reflect the views of the publisher.

Acknowledgements. We thank SURF for the support in using the National Supercomputer Snellius. We also thank José A. A. Antolínez (TU Delft) for discussions that helped in this research, Robyn Gwee (National University of Singapore) for sharing examples of prior GTSM data processing that was developed further in this work, and Kun Yan (Deltares) for support in making the data available through the C3S Climate Data Store.

Financial support. This research has been supported by the Nederlandse Organisatie voor Wetenschappelijk Onderzoek (grant no. OCENW.M.21.109).

Review statement. This paper was edited by Guillaume Charria and reviewed by two anonymous referees.

References

Arns, A., Wahl, T., Wolff, C., Vafeidis, A. T., Haigh, I. D., Woodworth, P., Niehüser, S., and Jensen, J.: Nonlinear interaction modulates global extreme sea levels, coastal flood exposure, and impacts, Nat. Commun., 11, 1918, https://doi.org/10.1038/s41467-020-15752-5, 2020.

Bell, B., Hersbach, H., Simmons, A., Berrisford, P., Dahlgren, P., Horányi, A., Muñoz-Sabater, J., Nicolas, J., Radu, R., Schepers, D., Soci, C., Villaume, S., Bidlot, J., Haimberger, L., Woollen, J., Buontempo, C., and Thépaut, J.: The ERA5 global reanalysis: Preliminary extension to 1950, Q. J. Roy. Meteor. Soc., 147, 4186–4227, https://doi.org/10.1002/qj.4174, 2021.

Bloemendaal, N., Muis, S., Haarsma, R. J., Verlaan, M., Irazoqui Apecechea, M., De Moel, H., Ward, P. J., and Aerts, J. C. J. H.: Global modeling of tropical cyclone storm surges using high-resolution forecasts, Clim. Dynam., 52, 5031–5044, https://doi.org/10.1007/s00382-018-4430-x, 2019.

Bloemendaal, N., De Moel, H., Muis, S., Haigh, I. D., and Aerts, J. C.: Estimation of global tropical cyclone wind speed probabilities using the STORM dataset, Sci. Data, 7, 377, https://doi.org/10.1038/s41597-020-00720-x, 2020.

Bocharov, G.: pyextremes, Version 2.4.0, GitHub [code], https://github.com/georgebv/pyextremes (last access: 22 July 2026), 2023.

Brown, S., Nicholls, R., Goodwin, P., Haigh, I., Lincke, D., Vafeidis, A., and Hinkel, J.: Quantifying Land and People Exposed to Sea-Level Rise with No Mitigation and 1.5 °C and 2.0 °C Rise in Global Temperatures to Year 2300, Earths Future, 6, https://doi.org/10.1002/2017ef000738, 2018.

Camus, P., Haigh, I. D., Nasr, A. A., Wahl, T., Darby, S. E., and Nicholls, R. J.: Regional analysis of multivariate compound coastal flooding potential around Europe and environs: sensitivity analysis and spatial patterns, Nat. Hazards Earth Syst. Sci., 21, 2021–2040, https://doi.org/10.5194/nhess-21-2021-2021, 2021.

Carrère, L., Lyard, F., Cancet, M., Guillot, A., and Roblou, L.: FES 2012: a new global tidal model taking advantage of nearly 20 years of altimetry, in Proceedings of "20 Years of Progress in Radar Altimetry", Venice, Italy, 26–29 September 2012, ISBN 978-92-9221-274-2, 2012.

Charnock, H.: Wind stress on a water surface, Q. J. Roy. Meteor. Soc., 81, 639–640, https://doi.org/10.1002/qj.49708135027, 1955.

Couasnon, A., Eilander, D., Muis, S., Veldkamp, T. I. E., Haigh, I. D., Wahl, T., Winsemius, H. C., and Ward, P. J.: Measuring compound flood potential from river discharge and storm surge extremes at the global scale, Nat. Hazards Earth Syst. Sci., 20, 489–504, https://doi.org/10.5194/nhess-20-489-2020, 2020.

Dulac, W., Cattiaux, J., Chauvin, F., Bourdin, S., and Fromang, S.: Assessing the representation of tropical cyclones in ERA5 with the CNRM tracker, Clim. Dynam., 62, 223–238, https://doi.org/10.1007/s00382-023-06902-8, 2024.

Dullaart, J. C. M., Muis, S., Bloemendaal, N., and Aerts, J. C. J. H.: Advancing global storm surge modelling using the new ERA5 climate reanalysis, Clim. Dynam., 54, 1007–1021, https://doi.org/10.1007/s00382-019-05044-0, 2020.

Eilander, D., Couasnon, A., Ikeuchi, H., Muis, S., Yamazaki, D., Winsemius, H. C., and Ward, P. J.: The effect of surge on riverine flood hazard and impact in deltas globally, Environ. Res. Lett., 15, 104007, https://doi.org/10.1088/1748-9326/ab8ca6, 2020.

EMODnet Bathymetry Consortium: EMODnet Digital Bathymetry (DTM 2018), EMODnet Bathymetry Consortium [data set], https://doi.org/10.12770/18FF0D48-B203-4A65-94A9-5FD8B0EC35F6, 2018.

Enríquez, A. R., Wahl, T., Marcos, M., and Haigh, I. D.: Spatial Footprints of Storm Surges Along the Global Coastlines, J. Geophys. Res.-Oceans, 125, e2020JC016367, https://doi.org/10.1029/2020JC016367, 2020.

Fang, J., Sun, S., Shi, P., and Wang, J.: Assessment and Mapping of Potential Storm Surge Impacts on Global Population and Economy, Int. J. Disast. Risk Sc., 5, 323–331, https://doi.org/10.1007/s13753-014-0035-0, 2014.

Fretwell, P., Pritchard, H. D., Vaughan, D. G., Bamber, J. L., Barrand, N. E., Bell, R., Bianchi, C., Bingham, R. G., Blankenship, D. D., Casassa, G., Catania, G., Callens, D., Conway, H., Cook, A. J., Corr, H. F. J., Damaske, D., Damm, V., Ferraccioli, F., Forsberg, R., Fujita, S., Gim, Y., Gogineni, P., Griggs, J. A., Hindmarsh, R. C. A., Holmlund, P., Holt, J. W., Jacobel, R. W., Jenkins, A., Jokat, W., Jordan, T., King, E. C., Kohler, J., Krabill, W., Riger-Kusk, M., Langley, K. A., Leitchenkov, G., Leuschen, C., Luyendyk, B. P., Matsuoka, K., Mouginot, J., Nitsche, F. O., Nogi, Y., Nost, O. A., Popov, S. V., Rignot, E., Rippin, D. M., Rivera, A., Roberts, J., Ross, N., Siegert, M. J., Smith, A. M., Steinhage, D., Studinger, M., Sun, B., Tinto, B. K., Welch, B. C., Wilson, D., Young, D. A., Xiangbin, C., and Zirizzotti, A.: Bedmap2: improved ice bed, surface and thickness datasets for Antarctica, The Cryosphere, 7, 375–393, https://doi.org/10.5194/tc-7-375-2013, 2013.

Ghanavati, M., Young, I., Kirezci, E., Ranasinghe, R., Duong, T. M., and Luijendijk, A. P.: An assessment of whether long-term global changes in waves and storm surges have impacted global coastlines, Sci. Rep.-UK, 13, 11549, https://doi.org/10.1038/s41598-023-38729-y, 2023.

Haigh, I. D., Marcos, M., Talke, S. A., Woodworth, P. L., Hunter, J. R., Hague, B. S., Arns, A., Bradshaw, E., and Thompson, P.: GESLA Version 3: A major update to the global higher-frequency sea-level dataset, Geosci. Data J., 10, 293–314, https://doi.org/10.1002/gdj3.174, 2023.

Hersbach, H., Bell, B., Berrisford, P., Biavati, G., Horanyi, A., Munoz Sabater, J., Nicolas, J., Peubey, C., Radu, R., Rozum, I., Schepers, D., Simmons, A., Soci, C., Dee, D., and Thepaut, J.-N.: ERA5 hourly data on single levels from 1940 to present, Copernicus Climate Change Service (C3S) Climate Data Store (CDS) [data set], https://doi.org/10.24381/CDS.ADBB2D47, 2023.

Hinkel, J., Lincke, D., Vafeidis, A., Perrette, M., Nicholls, R., Tol, R., Marzeion, B., Fettweis, X., Ionescu, C., and Levermann, A.: Coastal flood damage and adaptation cost under 21st century sea-level rise, P. Natl. Acad. Sci. USA, 111, 3292–3297, https://doi.org/10.1073/pnas.1222469111, 2014.

Hinkel, J., Feyen, L., Hemer, M., Le Cozannet, G., Lincke, D., Marcos, M., Mentaschi, L., Merkens, J., Moel, H., Muis, S., Nicholls, R., Vafeidis, A., Wal, R. S. W., Vousdoukas, M., Wahl, T., Ward, P., and Wolff, C.: Uncertainty and Bias in Global to Regional Scale Assessments of Current and Future Coastal Flood Risk, Earths Future, 9, https://doi.org/10.1029/2020EF001882, 2021.

Hoyer, S. and Hamman, J.: xarray: N-D labeled Arrays and Datasets in Python, Journal of Open Research Software, 5, https://doi.org/10.5334/jors.148, 2017.

Ikeuchi, H., Hirabayashi, Y., Yamazaki, D., Muis, S., Ward, P. J., Winsemius, H. C., Verlaan, M., and Kanae, S.: Compound simulation of fluvial floods and storm surges in a global coupled river-coast flood model: Model development and its application to 2007 Cyclone Sidr in Bangladesh, J. Adv. Model. Earth Sy., 9, 1847–1862, https://doi.org/10.1002/2017MS000943, 2017.

IPCC: Climate Change 2013: The Physical Science Basis. Contribution of Working Group I to the Fifth Assessment Report of the Intergovernmental Panel on Climate Change, edited by: Stocker, T. F., Qin, D., Plattner, G.-K., Tignor, M., Allen, S. K., Boschung, J., Nauels, A., Xia, Y., Bex, V., and Midgley, P. M., Cambridge University Press, Cambridge, United Kingdom, https://doi.org/10.1017/CBO9781107415324, 2013.

Kernkamp, H. W. J., Van Dam, A., Stelling, G. S., and De Goede, E. D.: Efficient scheme for the shallow water equations on unstructured grids with application to the Continental Shelf, Ocean Dynam., 61, 1175–1188, https://doi.org/10.1007/s10236-011-0423-6, 2011.

Kirezci, E., Young, I. R., Ranasinghe, R., Muis, S., Nicholls, R. J., Lincke, D., and Hinkel, J.: Projections of global-scale extreme sea levels and resulting episodic coastal flooding over the 21st Century, Sci. Rep.-UK, 10, 11629, https://doi.org/10.1038/s41598-020-67736-6, 2020.

Koks, E. E., Le Bars, D., Essenfelder, A. H., Nirandjan, S., and Sayers, P.: The impacts of coastal flooding and sea level rise on critical infrastructure: a novel storyline approach, Sustainable and Resilient Infrastructure, 8, 237–261, https://doi.org/10.1080/23789689.2022.2142741, 2023.

Le Bars, D.: Uncertainty in Sea Level Rise Projections Due to the Dependence Between Contributors, Earths Future, 6, 1275–1291, https://doi.org/10.1029/2018EF000849, 2018.

Li, H., Haer, T., Couasnon, A., Enríquez, A. R., Muis, S., and Ward, P. J.: A spatially-dependent synthetic global dataset of extreme sea level events, Weather and Climate Extremes, 41, 100596, https://doi.org/10.1016/j.wace.2023.100596, 2023.

Lin, N. and Emanuel, K.: Grey swan tropical cyclones, Nat. Clim. Change, 6, 106–111, https://doi.org/10.1038/nclimate2777, 2016.

Lincke, D. and Hinkel, J.: Economically robust protection against 21st century sea-level rise, Global Environ. Chang., 51, 67–73, https://doi.org/10.1016/j.gloenvcha.2018.05.003, 2018.

Lobeto, H. and Menendez, M.: Variability Assessment of Global Extreme Coastal Sea Levels Using Altimetry Data, Remote Sens.-Basel, 16, 1355. https://doi.org/10.3390/rs16081355, 2024.

Menéndez, M. and Woodworth, P. L.: Changes in extreme high water levels based on a quasi-global tide-gauge data set, J. Geophys. Res., 115, 2009JC005997, https://doi.org/10.1029/2009JC005997, 2010.

Muis, S., Verlaan, M., Winsemius, H. C., Aerts, J. C. J. H., and Ward, P. J.: A global reanalysis of storm surges and extreme sea levels, Nat. Commun., 7, 11969, https://doi.org/10.1038/ncomms11969, 2016.

Muis, S., Verlaan, M., Nicholls, R., Brown, S., Hinkel, J., Lincke, D., Vafeidis, A., Scussolini, P., Winsemius, H., and Ward, P.: A comparison of two global datasets of extreme sea levels and resulting flood exposure, Earths Future, 5, https://doi.org/10.1002/2016EF000430, 2017.

Muis, S., Haigh, I. D., Guimarães Nobre, G., Aerts, J. C. J. H., and Ward, P. J.: Influence of El Niño-Southern Oscillation on Global Coastal Flooding, Earths Future, 6, 1311–1322, https://doi.org/10.1029/2018EF000909, 2018.

Muis, S., Irazoqui, M., Dullaart, J., Rego, J., Madsen, K., Su, J., Yan, K., and Verlaan, M.: A High-Resolution Global Dataset of Extreme Sea Levels, Tides, and Storm Surges, Including Future Projections, Frontiers in Marine Science, 7, 263, https://doi.org/10.3389/fmars.2020.00263, 2020.

Muis, S., Aerts, J. C. J. H., Antolínez, J. A. Á., Dullaart, J. C., Duong, T. M., Erikson, L., Haarsma, R. J., Apecechea, M. I., Mengel, M., Le Bars, D., O'Neill, A., Ranasinghe, R., Roberts, M. J., Verlaan, M., Ward, P. J., and Yan, K.: Global Projections of Storm Surges Using High-Resolution CMIP6 Climate Models, Earths Future, 11, e2023EF003479, https://doi.org/10.1029/2023EF003479, 2023a.

Muis, S., Irazoqui Apecechea, M., and Bars, D. L.: Mean sea level fields used within the GTSMip simulations, Zenodo [data set], https://doi.org/10.5281/ZENODO.3948088, 2023b.

Muis, S., Irazoqui Apecechea, M., Antolinez, J. A. Á., Verlaan, M., Yan, K., Dullaart, J., Aerts, J. C. J. H., Duong, T., Ranasinghe, R., Le Bars, D., Haarsma, R. J., and Roberts, M.: Global sea level change time series from 1950 to 2050 derived from reanalysis and high resolution CMIP6 climate projections, https://doi.org/10.24381/CDS.A6D42D60, 2025a.

Muis, S., Aleksandrova, N., Veenstra, J., and Gwee, R.: GTSM-ERA5-E dataset – Data underlying the paper "Global dataset of storm surges and extreme sea levels for 1950–2024 based on the ERA5 climate reanalysis", Zenodo [data set], https://doi.org/10.5281/ZENODO.14671593, 2025b.

Nasr, A. A., Wahl, T., Rashid, M. M., Camus, P., and Haigh, I. D.: Assessing the dependence structure between oceanographic, fluvial, and pluvial flooding drivers along the United States coastline, Hydrol. Earth Syst. Sci., 25, 6203–6222, https://doi.org/10.5194/hess-25-6203-2021, 2021.

Reimann, L., Vafeidis, A. T., Brown, S., Hinkel, J., and Tol, R. S. J.: Mediterranean UNESCO World Heritage at risk from coastal flooding and erosion due to sea-level rise, Nat. Commun., 9, 4161, https://doi.org/10.1038/s41467-018-06645-9, 2018.

Ridder, N. N., Pitman, A. J., Westra, S., Ukkola, A., Do, H. X., Bador, M., Hirsch, A. L., Evans, J. P., Di Luca, A., and Zscheischler, J.: Global hotspots for the occurrence of compound events, Nat. Commun., 11, 5956, https://doi.org/10.1038/s41467-020-19639-3, 2020.

Stolte, W., Baart, F., Muis, S., Hijma, M., Taal, M., Le Bars, D., and Drijfhout, S.: Zeespiegelmonitor 2022, Report, Deltares, https://open.rijkswaterstaat.nl/@261752/zeespiegelmonitor-2022/ (last access: 22 July 2026), 2023.

Tadesse, M. G., Wahl, T., Rashid, M. M., Dangendorf, S., Rodríguez-Enríquez, A., and Talke, S. A.: Long-term trends in storm surge climate derived from an ensemble of global surge reconstructions, Sci. Rep.-UK, 12, 13307, https://doi.org/10.1038/s41598-022-17099-x, 2022.

Tiggeloven, T., de Moel, H., Winsemius, H. C., Eilander, D., Erkens, G., Gebremedhin, E., Diaz Loaiza, A., Kuzma, S., Luo, T., Iceland, C., Bouwman, A., van Huijstee, J., Ligtvoet, W., and Ward, P. J.: Global-scale benefit–cost analysis of coastal flood adaptation to different flood risk drivers using structural measures, Nat. Hazards Earth Syst. Sci., 20, 1025–1044, https://doi.org/10.5194/nhess-20-1025-2020, 2020.

Treu, S., Muis, S., Dangendorf, S., Wahl, T., Oelsmann, J., Heinicke, S., Frieler, K., and Mengel, M.: Reconstruction of hourly coastal water levels and counterfactuals without sea level rise for impact attribution, Earth Syst. Sci. Data, 16, 1121–1136, https://doi.org/10.5194/essd-16-1121-2024, 2024.

Veenstra, J.: Hatyan: Tidal Analysis and Prediction. Version v2.14.0, Zenodo [code], https://doi.org/10.5281/zenodo.19236057, 2026.

Verschuur, J., Koks, E. E., Li, S., and Hall, J. W.: Multi-hazard risk to global port infrastructure and resulting trade and logistics losses, Commun. Earth Environ., 4, 5, https://doi.org/10.1038/s43247-022-00656-7, 2023.

Wahl, T., Haigh, I. D., Nicholls, R. J., Arns, A., Dangendorf, S., Hinkel, J., and Slangen, A. B. A.: Understanding extreme sea levels for broad-scale coastal impact and adaptation analysis, Nat. Commun., 8, 16075, https://doi.org/10.1038/ncomms16075, 2017.

Weatherall, P., Marks, K. M., Jakobsson, M., Schmitt, T., Tani, S., Arndt, J. E., Rovere, M., Chayes, D., Ferrini, V., and Wigley, R.: A new digital bathymetric model of the world's oceans, Earth and Space Science, 2, 331–345, https://doi.org/10.1002/2015EA000107, 2015.

Woodworth, P. L., Melet, A., Marcos, M., Ray, R. D., Wöppelmann, G., Sasaki, Y. N., Cirano, M., Hibbert, A., Huthnance, J. M., Monserrat, S., and Merrifield, M. A.: Forcing Factors Affecting Sea Level Changes at the Coast, Surv. Geophys., 40, 1351–1397, https://doi.org/10.1007/s10712-019-09531-1, 2019.